Journal of Applied and Natural Science
14(2), 566 - 574 (2022)
ISSN : 0974-9411 (Print), 2231-5209 (Online)
journals.ansfoundation.org

Research Article

Spatial and temporal estimation of actual evapotranspiration of lower Bhavani basin, Tamil Nadu using Surface Energy Balance Algorithm for Land Model

C. G. Karishma
Department of Soil and Water Conservation Engineering, AEC&RI, Tamil Nadu Agricultural University, Coimbatore - 641003 (Tamil Nadu) India
Balaji Kannan*
Department of Soil and Water Conservation Engineering, Tamil Nadu Agricultural University, Coimbatore- 641003 (Tamil Nadu) India
K. Nagarajan
Department of Soil and Water Conservation Engineering, Tamil Nadu Agricultural University, Coimbatore - 641003 (Tamil Nadu) India
S. Panneerselvam
Water Technology Center, Tamil Nadu Agricultural IUniversity, Coimbatore - 641003 (Tamil Nadu) India
S. Pazhanivelan
Department of Remote Sensing and GIS, Tamil Nadu Agricultural University, Coimbatore - 641003 (Tamil Nadu) India

*Corresponding author. Email: balajikannan73@gmail.com

Article Info
https://doi.org/10.31018/jans.v14i2.3412
Received: March 27, 2022
Revised: May 30, 2022
Accepted: June 7, 2022

How to Cite
Karishma, C. G. *et al.* (2022). Spatial and temporal estimation of actual evapotranspiration of lower Bhavani basin, Tamil Nadu using Surface Energy Balance Algorithm for Land Model. *Journal of Applied and Natural Science*, 14(2), 566 - 574. https://doi.org/10.31018/jans.v14i2.3412

Abstract
Estimating evapotranspiration's spatiotemporal variance is critical for regional water resource management and allocation, including irrigation scheduling, drought monitoring, and forecasting. The Surface Energy Balance Algorithm for Land (SEBAL) method can be used to estimate spatio-temporal variations in evapotranspiration (ET) using remote sensing-based variables like Land Surface Temperature (LST), Normalized Difference Vegetation Index (NDVI), surface albedo, transmittance, and surface emissivity. The main aim of the study was to evaluate the actual evapotranspiration for the lower Bhavani basin, Tamil Nadu based on remote sensing methods using Landsat 8 data for the years 2018 to 2020. The actual evapotranspiration was estimated using SEBAL model and its spatial variation was compared over different land covers. The estimated values of daily actual evapotranspiration in the lower Bhavani basin ranged from 0 to 4.72 mm day^{-1}. Thus it is evident that SEBAL model can be used to predict ET with limited ground base hydrological data. The spatially estimated ET values will help in managing the crop water requirement at each stage of crop and irrigation scheduling, which will ensure the efficient use of available water resources.

Keywords: Actual evapotranspiration, Remote sensing, Spatio-temporal, Surface Energy Balance Algorithm for Land

INTRODUCTION

Evapotranspiration is a vital component of the global water cycle and offers a critical relationship concerning carbon, terrestrial water and surface energy exchanges. Evapotranspiration is extremely hard to quantify and forecast particularly at large -spatial scales. Estimating evapotranspiration's spatiotemporal variance is critical for regional water resource management and allocation, including irrigation scheduling, drought monitoring, and forecasting (Lian and Huang, 2016).

Most of the conventional and traditional methods are capable of providing accurate evapotranspiration measurements for a homogeneous region around a meteorological station, which cannot be extended or extrapolated to other areas (Liou and Kar, 2014). But with the help of remote sensing technology this has become feasible from a technical and economical point

of view. Remote sensing techniques allow for filling in the gap in providing the much-required spatially observed data (Rawat *et al*., 2019). Significant advances in remote sensing techniques, along with the availability of satellite images, have enabled alternative and accurate approaches for estimating evapotranspiration at regional scales (Mao and Wang, 2017).

Several methods have been developed at various spatial and temporal scales to estimate evapotranspiration. These methods ranges from semi-empirical /statistical / direct approaches to more analytical methods with a physical base in complexity as well as in numerical models simulating the heat and water flux through the atmosphere, vegetation, and soil. Remotely sensed data and methods have been utilized and assessed that provides the data required for estimation of ET using energy balance equation on pixel by pixel basis as well as the spatial variability of Evapotranspiration based on reflection; surface temperature; and net radiation (Mohamed *et al*., 2020).

Using satellite images, many algorithms have been developed to more precisely estimate ET (Allen *et al*., 2007).However, the Surface Energy Balance Algorithm for Land (SEBAL) (Bastiaanssen *et al*., 1998a) appears to be the most promising because it predicts Evapotranspiration at regional scale using very little amount of ground-based meteorological data and does not require a crop classification map (Bashir *et al*., 2008). SEBAL is one of the most widely used energy budgeting approaches for estimating actual evapotranspiration using satellite data (Bastiaanssen *et al*., 1998b). It uses local weather data and satellite data inputs to integrate empirical and physical parameterization (radiance). Normalized Difference Vegetation Index (NDVI), albedo , R (net solar radiation),G (soil heat flux) and, roughness length are all computed from the input data. The sensible heat flux is estimated by comparing two points designated as ' Cold' (wet) and ' hot ' pixels (dry barren ground). Then, the ET was computed as the residual of the energy budget (Bastiaanssen, 1998b, 2005). The SEBAL model has recognized to evaluate actual evapotranspiration with better accuracy. Its registered accuracies of 85% on a farm-scale while more than 95% accuracy was recorded on a regional scale (Seneviratne *et al*. 2006). Fawzy et al. (2021) used Landsat satellite data with the SEBAL algorithm to study daily evapotranspiration in the Nile Delta, Egypt, and reported that the SEBAL method estimated the transpiration evaporation of the region with acceptable accuracy. The purpose of this study was to compute the actual evapotranspiration (ET) from SEBAL using Landsat 8 images in the the lower bhavani basin, Tamil Nadu.

MATERIALS AND METHODS

Study area

This study was carried out in the Lower Bhavani basin is located in Tamil Nadu, and includes sections of Erode, Coimbatore, and Tirupur districts. The basin's overall geographical area is 2402 km^2, with latitudes ranging from 11° 15′ and 11° 45′ north and longitudes ranging from 77° 0′ and 77° 40′ east (Fig. 1). In terms of mean sea level, the ground elevation ranges between

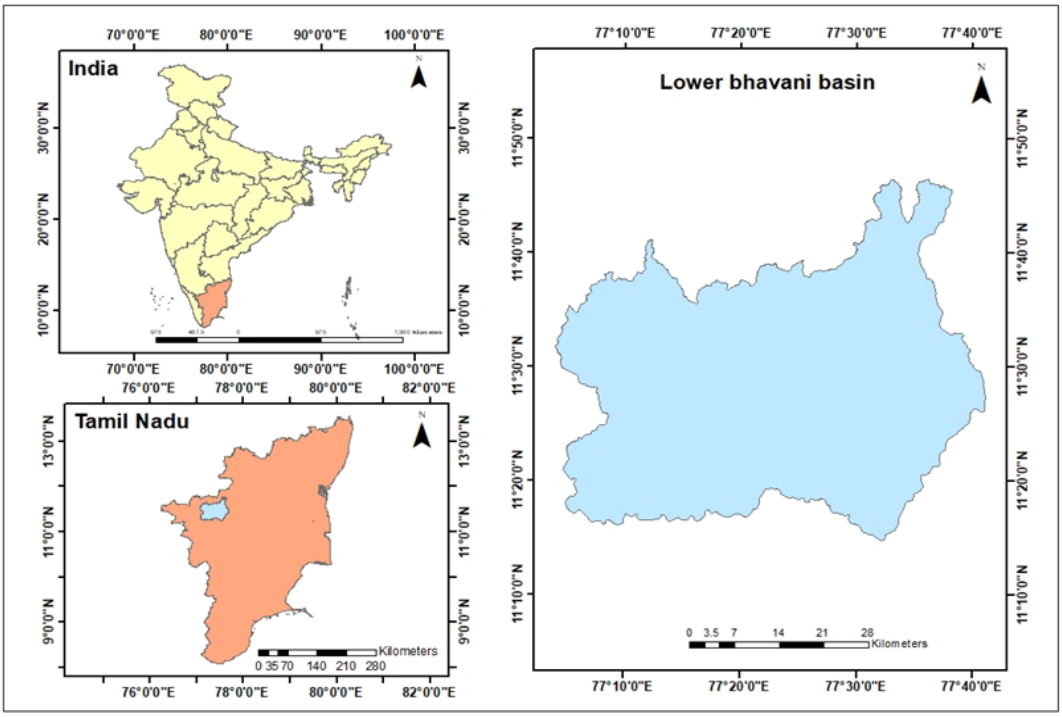

Fig. 1. *Study area map of lower Bhavani basin*

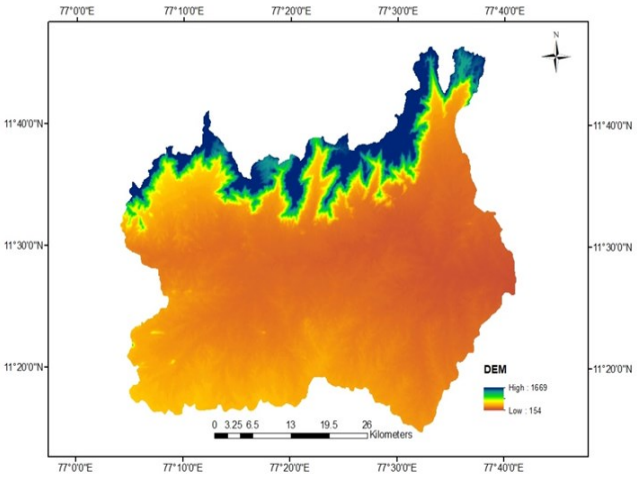

Fig. 2. *Digital elevation model of lower Bhavani basin (meters)*

154 and 1669 metres. The basin's regional slope is to the southeast. The climate in the area wawas semi-arid, with an average rainfall of 666.84 mm and temperatures ranging from 22 to 42 degrees Celsius

Weather data

Weather data such as Minimum and Maximum Temperature, Wind Speed, Relative Humidity, Sunshine hours was obtained from Agro Climate Research Centre, Tamil Nadu Agricultural University.

Digital elevation model (DEM) data

DEM data from Shuttle Radar Topographic Mission (SRTM) having spatial resolution of 30 m were downloaded from USGS Earth Explorer (www.earthexplorer.usgs.gov) for the lower Bhavani basin (Fig. 2).

Land use classification

The major land use classes were derived using Landsat 8 imagery by performing supervised classification technique in Google Earth Engine; five LULC classes were selected Agriculture; Builtup; Current Fallow; Forest and Water body. The classifiers trained using the training points. The CART and RF classifiers were used in GEE to perform the LULC classification.

Landsat 8 data

Ten different Landsat 8 images, path 144 and row 52 acquired from USGS earth explorer. The study was conducted for two growing seasons (2018-2020). The image acquisition date, solar elevation angle and zenith angle for the Landsat 8 data products used in this study are presented in Table 1. The images were selected such that there is no or minimum cloud cover in order to avoid error in calculation. The time series for Landsat 8 is 16 days and the spatial resolution is 30 m.

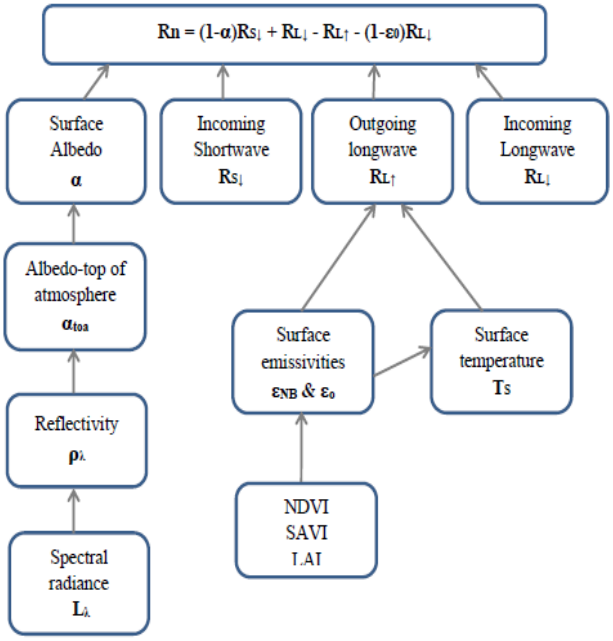

Fig. 3. *Flowchart for computation of net radiation*

SEBAL model

The SEBAL based daily Actual ET was estimated using different remote - sensing-based variables like net radiation, soil heat flux, sensible heat flux, latent heat flux, and and evaporative fraction using the python code developed and executed in Arcpy. Individual satellite images were processed using the SEBAL method, and maps of AET were prepared for each date.

The surface energy balance equation used in the the estimation of evapotranspiration is as follows (Bastiaanssen *et al*., 1998b):

$$\lambda ET = R_n - G - H \quad \text{Eq. 1}$$

Where; R_n is the net radiation flux at the surface (W/m^2); G is the soil heat flux (W/m^2); λET is the latent heat flux (W/m^2); and H is the sensible heat flux to the air (W/m^2). The coefficient λ is the latent heat of vapori-

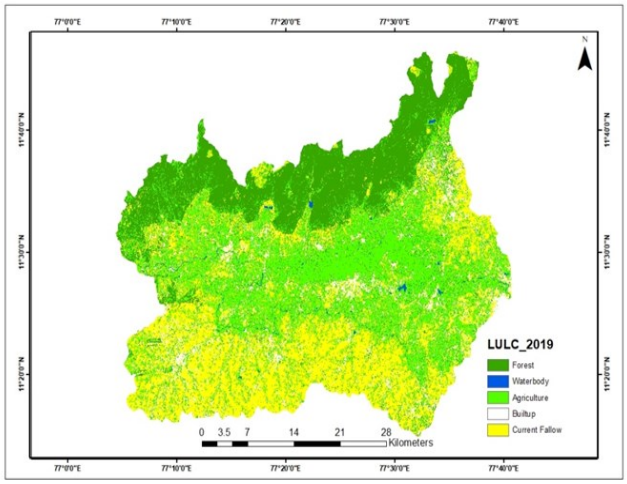

Fig. 4. *Land use map of lower Bhavani basin*

zation of water and ET is the vapor flux density in kg m^{-2} s^{-1}.

Net radiation

To compute the net radiation the following surface radiation balance equation is used:

$R_n = (1 - \alpha)_{\downarrow} + R_{L\downarrow} - R_{L\uparrow} - (1 - \varepsilon_0) R_{L\downarrow}$ Eq. 2

where α is surface albedo, $R_{L\downarrow}$ is incoming longwave radiation (W/m^2), $R_{s\downarrow}$ is incoming shortwave radiation (W/m^2), $R_{L\uparrow}$ is outgoing longwave radiation (W/m^2),and ε_0 is surface emissivity. The individual terms of net radiation are estimated as follows and depicted in Fig 3,

Surface albedo (α)

Surface albedo is defined as the ratio of the reflected radiation to the incident shortwave radiation. It is computed in SEBAL through the following equation:

$a = (a_{toa} - a_{atm}) / t^2$ Eq. 3

The atmospheric transmittance is a function of elevation and computed using the following equation:

$t = 0.75 + (2 \times 10^{-5} \times z)$ Eq. 4

where; z is the elevation extracted from the digital elevation model (DEM) for the study area (Fig. 2)

Incoming Shortwave Radiation ($R_{S\downarrow}$)

$R_{S\downarrow}$ is the direct and diffuse solar radiation flux that actually reaches the earth's surface (W/m^2). It is calculated using:

$R_{s\downarrow} = G_{sc} \times \cos\theta \times dr \times \tau_{sw}$ Eq. 5

where; G_{sc} is the solar constant (1367 W/m^2), cos θ is the cosine of the solar incidence angle, dr is the inverse squared relative earth-sun distance, and τ_{sw} is the atmospheric transmissivity. This calculation is done with a spreadsheet. Values of Incoming shortwave radiation can be from 200 to 1000 W/m^2 depending on the location and time of the satellite image.

Outgoing longwave radiation ($R_{L\uparrow}$)

$R_{L\uparrow}$ from the earth's surface to the atmosphere (W/m^2) is the $R_{L\uparrow}$. In SEBAL, it's calculated as a function of vegetation indices, surface emissivity and surface temperature. Soil Adjusted Vegetation Index (SAVI), Normalized Difference Vegetation Index (NDVI), and Leaf Area Index (LAI) are computed using reflectivity values.

The NDVI is the ratio of the differences in reflectivities for the near-infrared band (ρ_5) and the red band (ρ_4) to their sum:

$NDVI = (\rho_5 - \rho_4) / (\rho_5 + \rho_4)$ Eq. 6

where; ρ_5 and ρ_4 are reflectivities for bands 5 and 4. The NDVI is a sensitive measure of green vegetation quantity and condition. NDVI scale ranges from -1 to +1. Green surfaces have a NDVI between 0 and 1, whereas water and clouds have NDVI values of less than zero.

The SAVI attempts to "subtract" the effects of background soil from NDVI so that effects of soil wetness are reduced in the index. It is calculated as:

$SAVI = (1 + L) (\rho_5 - \rho_4) / (L + \rho_5 + \rho_4)$ Eq. 7

where; L is a constant for SAVI. If L is zero, SAVI becomes equal to NDVI.

The LAI is the ratio of the total area of all leaves on a plant to the ground area represented by the plant. It is an indicator of biomass and canopy resistance. LAI is computed using the following empirical equation:

$LAI = - 1 \times (Ln ((0.84 - SAVI) / 0.65) / 0.91)$ Eq. 8

The maximum value for "LAI" is 6.00, which corresponds to a maximum "SAVI" of 0.687. Beyond SAVI = 0.687, the value for SAVI "saturates" with increasing LAI and does not change significantly.

Surface emissivity (ε) is the ratio of the thermal energy radiated by the surface to the thermal energy radiated by a blackbody at the same temperature. It is derived empirically from NDVI

Land surface temperature (Ts)

Ts deals with energy exchange between the earth surface and the environment. It was calculated from the thermal band (band 10) radiance values of the Landsat 8 image. The equation for estimation of surface temperature is:

$T_s = K_2 / \ln ((\varepsilon_s \times K_1) / \rho_b)$ Eq. 9

Where, ρ_b is the radiance of the thermal band (band

Table 1. Particulars of selected Landsat 8 data for lower Bhavani basin

S. No.	Acquisition date (dd/mm/yyy)	Solar elevation angle (degrees)	Solar azimuth angle (degrees)
1	21-01-2018	48.14	138.54
2	06-02-2018	50.64	133.09
3	22-02-2018	54.15	126.33
4	08-01-2019	47.12	142.09
5	25-02-2019	48.46	137.66
6	13-03-2019	58.81	116.28
7	14-04-2019	64.86	92.74
8	11-01-2020	47.29	141.51
9	27-01-2020	48.89	136.85
10	31-03-2020	62.97	103.38

10). The constants K_1 and K_2 for band 10 are 774.8853 and 1321.0789 which was taken for each dataset from the metadata file.

The outgoing longwave radiation ($R_{L\uparrow}$) is computed using the Stefan-Boltzmann equation:

$$R_{L\uparrow} = \varepsilon_o \times \sigma \times T_s^{\ 4} \quad \text{Eq. 10}$$

where; ε_o is the "broad-band" surface emissivity (dimensionless), σ is the Stefan Boltzmann constant (5.67×10^{-8} W/ m^2 /K^4), and T_s is the surface temperature (K) .Values for outgoing longwave radiation can range from 200 to 700 W/m^2 depending on time and location of the satellite image.

Incoming longwave radiation ($R_{L\downarrow}$)

The downward thermal radiation flux from the atmosphere (W/m^2) is the incoming longwave radiation. It is calculated by using the Stefan-Boltzmann equation:

$$R_{L\downarrow} = \varepsilon_a \times \sigma \times T_a^{\ 4} \quad \text{Eq. 11}$$

where; ε_a is the atmospheric emissivity (dimensionless), σ is the Stefan-Boltzmann constant (5.67×10^{-8} W/m^2 / K^4), and T_a is the near surface air temperature (K). Bastiaanssen (1998b)

$$\varepsilon_a = 0.85 \times (-\ln \tau_{sw})^{.09} \quad \text{Eq. 12}$$

where; τ_{sw} is the atmospheric transmissivity calculated

The surface albedo (α), outgoing longwave radiation ($R_{L\uparrow}$), and surface emissivity (ε_o) are input along with the incoming shortwave radiation ($R_{S\downarrow}$) and the incoming longwave radiation ($R_{L\downarrow}$). The R_n is computed. Values for R_n can range from 100 to 700 W/m^2, depending on the surface. This concludes the first step of the SEBAL procedure.

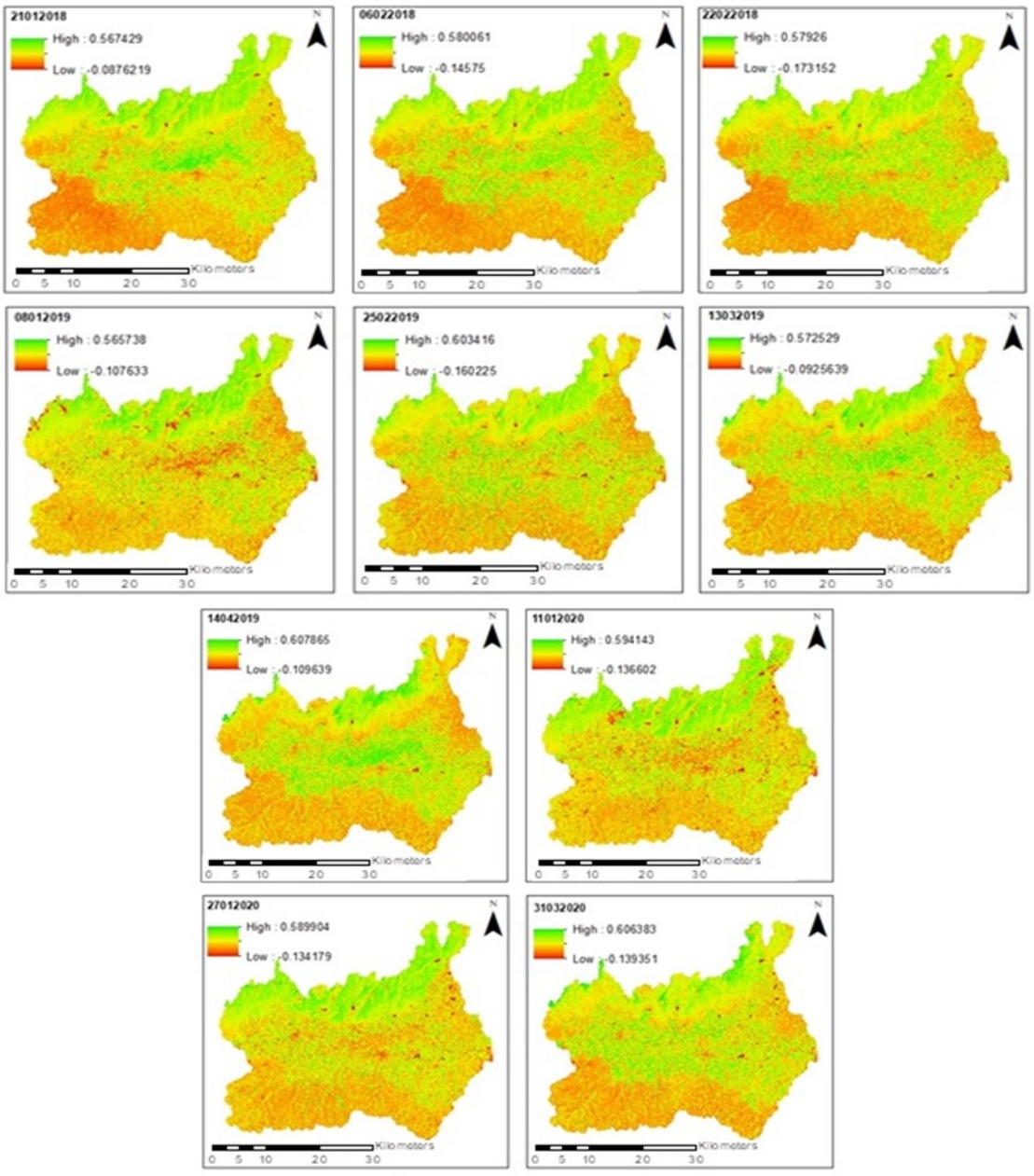

Fig. 5. *Variation of normalized difference vegetation index of lower Bhavani basin*

Table 2. Parameters obtained from SEBAL model

Image Date	NDVI	Albedo %	Ts (K)	R_N (W/m^2)	H (W/m^2)	G (W/m^2)	ET_{24} (mm/day)
21-01-2018	0.57	0.61	344.72	657.311	1034.01	184.108	4.72
06-02-2018	0.58	0.70	342.85	690.67	951.67	188.36	4.34
22-02-2018	0.58	0.72	342.58	717.03	800.95	196.89	4.13
08-01-2019	0.57	1.40	345.48	635.57	897.03	180.66	4.30
25-02-2019	0.60	0.84	349.58	738.87	732.23	218.16	4.34
13-03-2019	0.57	0.90	350.99	764.89	846.99	234.70	4.26
14-04-2019	0.61	0.95	355.13	821.01	844.27	269.56	4.30
11-01-2020	0.59	1.32	343.67	649.52	1233.6	175.52	4.69
27-01-2020	0.59	0.84	348.36	665.25	976.93	192.45	4.66
31-03-2020	0.61	0.82	352.03	808.05	919.95	252.07	4.16

Soil heat flux

The rate of heat energy transferred from the earth's surface to the subsurface is Soil heat flux. It is calculated using the following equation and is a function of the net radiation, surface temperature, albedo and normalized difference vegetation index (NDVI).

$$G = R_n\,(T_s\,(0.0038 + 0.0074\,\alpha)\,(1 - 0.978\,NDVI^{\,4}))$$ Eq. 13

Sensible heat flux

The rate of heat energy transmission from the earth's surface to the atmosphere via conduction and convection is known as sensible heat flux. Surface roughness, temperature gradient, and wind speed all influence the sensible heat flux. The sensible heat flux is calculated by SEBAL using the following equation:

$H = \rho\, c_p\, dT / r_{ah}$ Eq. 14

where ρ is the air density (kg/m^3), c_p is the specific heat of air at constant pressure (J/kg K), dT is the vertical near surface temperature difference (K) and r_{ah} is the aerodynamic resistance to heat transport (s/m).

To set boundary conditions for the energy balance, the SEBAL method uses two "anchor" pixels. These are the "hot" and "cold" pixels that are in the interest region. In a moist region, such as a waterbody, the "cold" pixel is chosen. At this pixel, the surface and near-surface air temperatures are expected to be identical.The "hot" pixel is selected as a dry, bare agricultural field where ET is assumed to be zero.

The aerodynamic resistance to heat transport (rah) is computed for neutral stability as:

$r_{ah} = \ln (z_2/z_1) / u^* \times k$ Eq. 15

where; z_1 and z_2 are heights in meters above the zero plane displacement (d) of the vegetation, u* is the friction velocity (m/s), and k is von Karman's constant which is 0.41. The friction velocity (u*) is calculated using the logarithmic wind law for neutral atmospheric conditions:

$u^* = k u_x / (\ln(z_x/z_{om}))$ Eq. 16

where; k is von Karman's constant, u_x is the wind speed (m/s) at height z_x, and z_{om} is the momentum roughness length (m). z_{om} is a measure of the form drag and skin friction for the layer of air that interacts with the surface.

Latent heat flux (λET)

Latent heat flux is the rate of latent heat loss from the surface due to evapotranspiration; the following equation was obtained from which latent heat flux was calculated.

$\lambda ET = R_n - H - G$ Eq. 17

where; λET is an instantaneous value for the time of the satellite overpass (W/m^2). Then instantaneous evaporative fraction was calculated by using the following equation

$f = \lambda ET / (R_n - G)$ Eq. 18

Daily actual evapotranspiration

Finally, daily actual ET_c was estimated by the following equation:

$ET_c = f \times (R_{n24} - G_{24}) / \rho_w \lambda$ Eq. 19

Where ET_c is daily crop ET (mm day^{-1}), R_{n24} is daily net radiation calculated on a daily time step (MJ s $^{-1}$ m^{-2}) and G_{24} is the daily soil heat flux which is taken as zero, ρ_w is the density of water and λ is the latent heat of vaporization (2.45 MJ kg^{-1}).

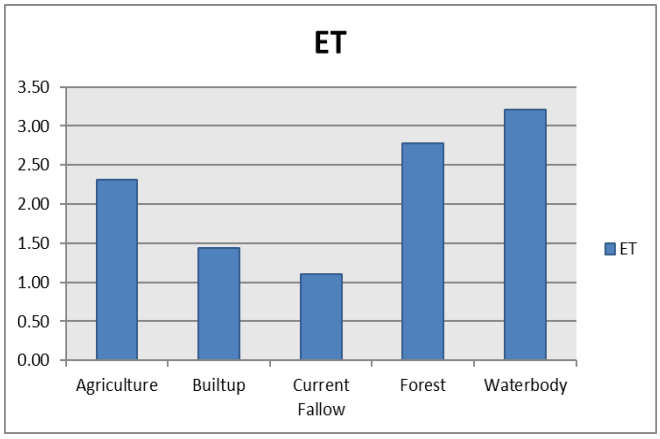

Fig. 6. *Spatial variation of actual evapotranspiration (ET) in different surfaces*

RESULTS AND DISCUSSION

Land use classification

The classified land use map presented in Fig.4. with an overall accuracy of 85% revealed that out of the 2400 km^2 of the area, the the agricultural area was 35.60%. Builtup and current fallow covered 7.37% and 30.07%,, respectively while forest 26.54%. The area covered by water bodies was 0.41%.

Normalized difference vegetation iindex

The spatial variation of NDVI in the the lower Bhavani basin for the yearss 2018, 2019 and 2020 are shown in Fig. 5. The NDVI values ranged from -0.08 to 0.58, -0.09 to 0.61 and -0.13 to 0.61, respectively. Higher NDVI values were observed for agricultural fields and forestss in the study area.

Actual evapotranspiration using SEBAL

SEBAL is selected because it is the most widely used model as it provides a robust and efficient tool for estimating the spatial distribution of ET. The use of a near surface temperature gradient dT, linked to the radiometric surface temperature, Ts, to obviate the necessity for absolute surface aerodynamic temperature calibration is the model's most distinguishing feature.The su-

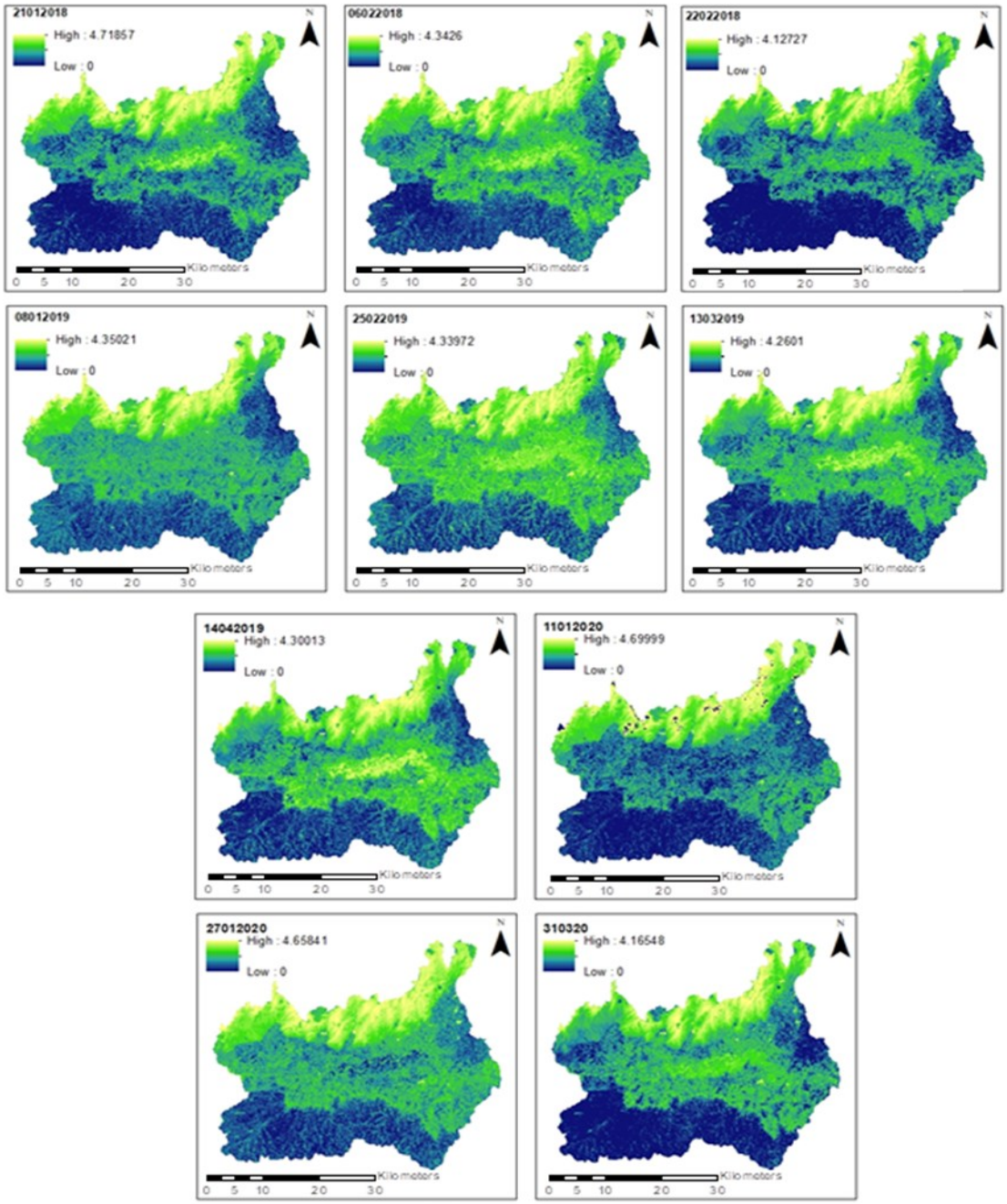

Fig. 7. *Variation of actual evapotranspiration of lower Bhavani basin (mm/day)*

periority of the SEBAL model over other approaches to estimate land surface fluxes from thermal remote sensing data is that it requires minimum auxiliary ground-based data, and it does not require a strict correction of atmospheric effects on surface temperature because of its automatic internal calibration.

As specified in Table 1, images from 2018 to 2020 were used. The values of the parameters obtained by the SEBAL algorithm for the lower BBhavani basin are presented in Table 2. The incoming longwave and shortwave radiations, which impact the surface temperature, directly dependimpact the surface temperature, directly depend on net solar radiation. As a result, locations with hotter surfaces get more net solar radiation. Firozjaei *et al*. (2019)) evaluated the energy balance parameters using SEBAL algorithm in the the city of Sari, Iran and inferred that the net radiation flux directly relates to the Greenness, NDVI, and Wetness parameters and is inversely linked to Brightness, albedo, and Ts, which is consistent with the findings. In the present study after calculating all the required parameters using the SEBAL algorithm indicated that the estimated values of daily Actual ET ranged from 0 to 4.72 mm day $^{-1}$ for the year 2018, from 0 to 4.35 mm day^{-1} for the year 2019 and from 0 to 4.70 mm day^{-1} for the year 2020 in the lower Bhavani basin, which was similar to the results reported by Jana *et al*. ((2016)) that actual evapotranspiration from SEBAL model was 4.9 mm day $^{-1}$ in Doon valley, India.

The computed SEBAL ET varied between 0 to 4.72 mm day^{-1} in lower BBhavani basin. Bala *et al*. (2017) also reported that average estimated ET using SEBAL model varied from 1.14 to 2.0 mm day^{-1} at the the early growth stage, 2.5 to 4 mm day^{-1} at the the middle growth stage and 3.0 to 4.5 mm day^{-1} at the the full growth stage of the wheat the crop in Hisar district.

The spatial and temporal variation of SEBAL actual evapotranspiration is given in Fig.7. The spatial variation of actual ET indicated for each land use is mentioned in Fig.6. Daily Actual ET increased from bare fallow land to the area with good and healthy crop cover as reflected in areas with higher values of vegetation indices. Furthermore, from the energy balance in in limiting cases, it is known that high rates of ET are physically possible when soil moisture is relatively high as the water body exhibit high AET. The area without crop, the area under exposed soil and built up area showed lower values of AET and higher values of LST.

Conclusion

The estimated values of daily actual evapotranspiration in the lower Bhavani basin ranged from 0 to 4.72 mm day^{-1}. Daily Actual ET variation increased from bare fallow land to the area with good and healthy crop cover as reflected in areas with higher values of vegetation indices. Thus it is evident that SEBAL model can be used to predict ET with limited ground base hydrological data. The spatially estimated ET values will help in managing the crop water requirement at each stage of crop and irrigation scheduling, which will ensure the efficient use of available water resources. The outcomes of this research will be valuable in the management of agricultural water resources.

ACKNOWLEDGEMENTS

The authors wish to express their gratitude to Tamil Nadu Agricultural University, Coimbatore.

Conflict of interest

The authors declare that they have no conflict of interest.

REFERENCES

1. Bastiaanssen, W. G. M. *et al*. 共2005夭. “SEBAL model with remotely sensed data to improve water-resources management under actual field conditions.” J. Irrig. Drain. Eng., 131共1夭, 85–93
2. Bastiaanssen, W. G. M. *et al*. 共2005夭. “SEBAL model with remotely sensed data to improve water-resources management under actual field conditions.” J. Irrig. Drain. Eng., 131共1夭, 85–93
3. Allen, R. G., Tasumi, M. & Trezza, R. (2007). Satellite-based energy balance for mapping evapotranspiration with internalized calibration (METRIC)—Model. *Journal of irrigation and drainage engineering*, *133*(4), 380-394.
4. Bala, A., Pawar, P. S., Misra, A. K. & Rawat, K. S. (2017). Estimation and validation of actual evapotranspiration for wheat crop using SEBAL model over Hisar District, Haryana, India. *Current Science*, 134-141.
5. Bashir, M. A., Hata, T., Tanakamaru, H., Abdelhadi, A. W. & Tada, A. (2008). Satellite-based energy balance model to estimate seasonal evapotranspiration for irrigated sorghum: a case study from the Gezira scheme, Sudan. *Hydrology and Earth System Sciences*, *12*(4), 1129-1139.
6. Bastiaanssen, W. G. M., Noordman, E. J. M., Pelgrum, H., Davids, G., Thoreson, B. P. & Allen, R. G. (2005). SEBAL model with remotely sensed data to improve water-resources management under actual field conditions. *Journal of irrigation and drainage engineering*, *131* (1), 85-93.
7. Bastiaanssen, W. G., Pelgrum, H., Wang, J., Ma, Y., Moreno, J. F., Roerink, G. J. & Van der Wal, T. (1998a). A remote sensing surface energy balance algorithm for land (SEBAL).: Part 2: Validation. *Journal of Hydrology*, *212*, 213-229.
8. Bastiaanssen, W. G., Menenti, M., Feddes, R. A. & Holtslag, A. A. M. (1998b). A remote sensing surface energy balance algorithm for land (SEBAL). 1. Formulation. *Journal of hydrology*, *212*, 198-212.
9. Fawzy, H. E. D., Sakr, A., El-Enany, M. & Moghazy, H. M.

(2021). Spatiotemporal assessment of actual evapotranspiration using satellite remote sensing technique in the Nile Delta,Egypt. *Alexandria Engineering Journal*, *60*(1), 1421-1432.

10. Firozjaei, M. K., Kiavarz, M., Nematollahi, O., Karimpour Reihan, M. & Alavipanah, S. K. (2019). An evaluation of energy balance parameters, and the relations between topographical and biophysical characteristics using the mountainous surface energy balance algorithm for land (SEBAL). *International Journal of Remote Sensing*, *40* (13), 5230-5260.
11. Lian, J. & Huang, M. (2016). Comparison of three remote sensing based models to estimate evapotranspiration in an oasis-desert region. *Agricultural Water Management*, *165*, 153-162.
12. Liou, Y. A. & Kar, S. K. (2014). Evapotranspiration estimation with remote sensing and various surface energy balance algorithms—A review. *Energies*, *7*(5), 2821-2849.
13. Mao, Y. & Wang, K. (2017). Comparison of evapotranspiration estimates based on the surface water balance, modified Penman□Monteith model, and reanalysis data sets for continental China. *Journal of Geophysical Research: Atmospheres*, *122*(6), 3228-3244.
14. Mohamed, E. S., Ali, A., El-Shirbeny, M., Abutaleb, K. & Shaddad, S. M. (2020). Mapping soil moisture and their correlation with crop pattern using remotely sensed data in arid region. *The Egyptian Journal of Remote Sensing and Space Science*, *23*(3), 347-353.
15. Rawat, K. S., Singh, S. K., Bala, A. & Szabo, S. (2019). Estimation of crop evapotranspiration through spatial distributed crop coefficient in a semi-arid environment. *Agricultural Water Management*, *213*, 922-933.
16. Seneviratne, S. I., Koster, R. D., Guo, Z., Dirmeyer, P. A., Kowalczyk, E., Lawrence, D.& Verseghy, D. (2006). Soil moisture memory in AGCM simulations: analysis of global land–atmosphere coupling experiment (GLACE) data. *Journal of Hydrometeorology*, *7*(5), 1090-1112.